Photopolarimetric Measurement System of Mueller Matrix
with Dual Rotating Waveplates

Kiyoshi Ichimoto, Kazuya Shinoda, Tetsuya Yamamoto[1], and Junko Kiyohara[2]

(Received October 24, 2005)

Abstract

A new photopolarimetric measurement system of Mueller matrix of optical elements is developed using dual rotating waveplates. The waveplates in polarization generator and analyzer rotate continuously with a constant radio of revolution speed, and the Mueller matrix of a sample can be obtained in a few seconds. General principle of such measurement and the optimization of operation parameters are discussed, followed by detailed descriptions of the constructed system. Some examples of its application are also demonstrated. The system is sensitive to $<10^{-3}$ for each Mueller matrix element for weak polarization elements.

Key words: optics, polarization, Mueller matrix, optical element

1. Introduction

Polarization of lights provides valuable information of the physical state of astronomical objects, especially it can provide information on vector quantities such as magnetic fields or radiation fields since the polarization of lights originates in anisotropical natures of the light source or the medium through which lights propagate. In the current solar research, the precise measurement of polarizations in atomic spectral lines is of a particular importance for obtaining the information of vector magnetic fields in the solar atmosphere, and, in general, an accuracy of 10^{-3} or higher is required in measurements.

For high precession polarimetory, it is essentially important to calibrate the instrumental polarization of the observing system with required accuracy (e.g. Makita et al. 1982). For this goal, characterization of optical components with Mueller matrices is the most suitable and commonly used approach. A new photopolarimetric system to measure the Mueller matrix of optical elements in a simple and convenient manner is constructed for the purpose of improving the calibration accuracy of existing polarimeters and to characterize the optical elements for new polarimetric instruments.

The Mueller matrix measurement system described in this paper consists of a polarization generator and a polarization analyzer with a sample to be measured in between them, and both of polarization generator and analyzer contain a rotating waveplate. The principle of such dual rotating waveplate system was studied earlier by Azzam (1978), where the formulations to deduce the Muller matrix elements are presented under the constraint in which both retarders are quarter waveplate and the ratio of angular speed is 1:5. Such system for real applications were constructed by, for examples, Goldstein (1992) for infrared polarimetory, and by Collins and Koh (1997) for spectroscopic polarimetory. The ratio of angular speeds of two waveplates are fixed at 1:5 in the former and 3:5 in the later case.

In this paper, we discuss the 'efficiency of measurement' based on general principle of the Mueller matrix measurement with dual rotating waveplates (section 2). The measurement system described in this paper is based on more general formalism and the ratio of the angular speed may not be fixed at particular value. The retardations and angle offsets of waveplates are self-calibrated by performing a 'clear' measurement without a sample in the optical path. Details of the hardware and reduction method of the constructed measurement system is described in section 3, and some examples of its application are demonstrated in section 4.

2. Principle of the Mueller Matrix Measurement with Dual Rotating Waveplates

Figure 1 shows the basic configuration of the system. The normalized intensity on the detector is expressed as follows;

$$I(\theta_1, \theta_2) = (1,0,0,0)\ \mathrm{PL}(\theta=0)\ \mathrm{WP}(\delta_1,\theta_1)\ \mathrm{M}\ \mathrm{WP}(\delta_2,\theta_2)\ \mathrm{PL}(\theta=0)\ (1,0,0,0)^t \quad (1)$$

where $(1,0,0,0)$ is the Stokes vector sensed by the detector, PLs are Mueller matrices of fixed linear polarizers in the polarization analyzer and the generator, $\mathrm{WP}(\delta_1, \theta_1)$ and $\mathrm{WP}(\delta_2, \theta_2)$ are Mueller matrices of rotating waveplates in polarization analyzer and generator respectively with $\delta_{1,2}$ and $\theta_{1,2}$ are their retardations and orientations, and M is the Mueller matrix of the sample to be determined by the measurement. The superscript t denotes the transpose. The ideal Mueller matrices of a polarizer and a linear retarder are given as followings;

(1) University of Tokyo, Hongo, Bunkyo-ku, Toyko, 113-0033, Japan

(2) Kwasan Observatory, Kyoto University, Kita-Kazan Ohmine-cho, Yamashina-ku, Kyoto, 607-8471, Japan

$$\mathbf{PL}(\theta) = \tfrac{1}{2}\,\mathbf{R}(-\theta) \cdot \begin{pmatrix} 1 & 1 & 0 & 0 \\ 1 & 1 & 0 & 0 \\ 0 & 0 & 0 & 0 \\ 0 & 0 & 0 & 0 \end{pmatrix} \cdot \mathbf{R}(\theta)$$

$$\mathbf{WP}(\delta,\theta) = \mathbf{R}(-\theta) \cdot \begin{pmatrix} 1 & 0 & 0 & 0 \\ 0 & 1 & 0 & 0 \\ 0 & 0 & \cos\delta & \sin\delta \\ 0 & 0 & -\sin\delta & \cos\delta \end{pmatrix} \cdot \mathbf{R}(\theta)$$

with the matrix of coordinate rotation

$$\mathbf{R}(\theta) = \begin{pmatrix} 1 & 0 & 0 & 0 \\ 0 & \cos 2\theta & \sin 2\theta & 0 \\ 0 & -\sin 2\theta & \cos 2\theta & 0 \\ 0 & 0 & 0 & 1 \end{pmatrix}$$

Equation (1) can be expressed with matrix elements as

$$I(\theta_1,\theta_2) = \sum_{k,l=1}^{4} c_{kl}(\theta_1,\theta_2) \cdot m_{kl} \qquad (2)$$

$$c_{kl}(\theta_1,\theta_2) \equiv \sum_{j,m=1}^{4} p^1{}_{1j}\, w^1{}_{jk}\, w^2{}_{lm}\, p^2{}_{m1}$$

where $p^1{}_{1j}$ and $p^2{}_{m1}$ are matrix elements of polarizer-1 and 2, $w^1{}_{jk}$ and $w^2{}_{lm}$ are of the waveplate-1 and 2, respectively. The 16 coefficients c_{kl} are shown as functions of θ_1 and θ_2 in figure 2, for the case of $\delta_1 = \delta_2 = 127°$ This plot demonstrates that each $c_{kl}(\theta_1, \theta_2)$ behaves as independent harmonics of θ_1 and θ_2; thus the Mueller matrix elements m_{kl} of the sample can be regarded as the Fourier components of the modulated intensity with respect to θ_1 and θ_2.
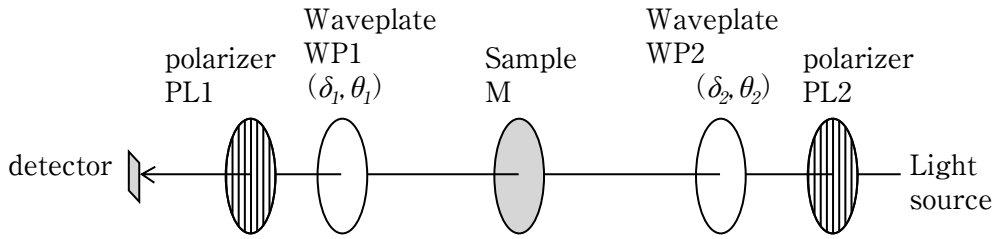

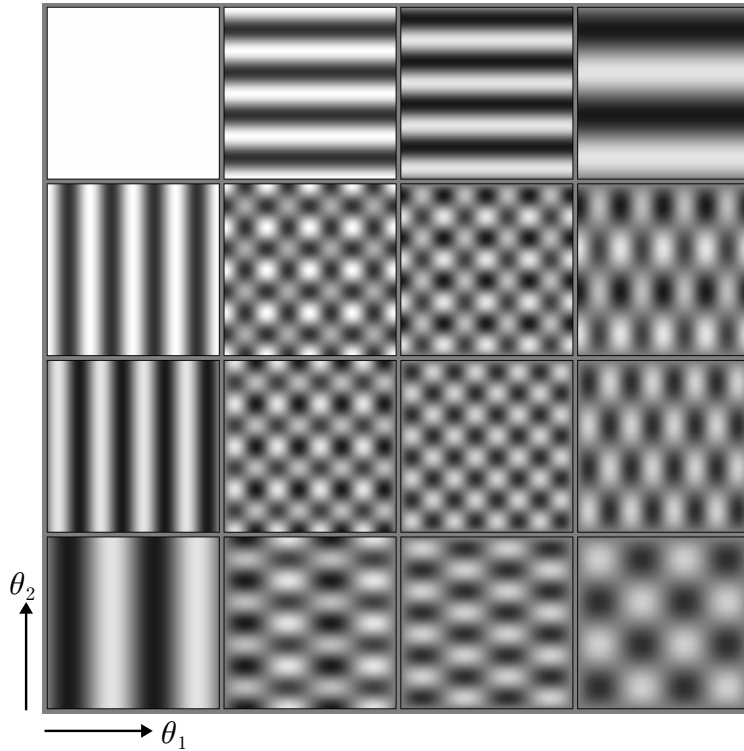Figure 1. Basic configuration of the Mueller matrix measurement system.

Figure 2. The 16 coefficients c_{kl} of the modulated intensity as functions of θ_1 and θ_2. Abscissa and ordinate of each box are θ_1 and θ_2 with a range from 0° to 360°.

Let us regard the c_{kl} and m_{kl} as a row and a column vectors with 16 elements respectively. Then equation (2) can be regarded as a scalar product of two vectors, and if we have N times measurements of I with different combinations of θ_1 and θ_2, equation (2) can further be written as

$$I = CM \qquad (3)$$

where **I** is a N-elements column vector of the measured intensity, **C** is a modulation matrix with 16xN elements, and **M** is a 16 element column vector. Equation (3) can be solved as

$$M = R\,I\,, \qquad R = (C^t C)^{-1} C^t \qquad (4)$$

where C^t is a transpose of **C**. Thus if the determinant of $C^t C$ is not zero, we can determine M from N times measurements of the modulated intensity. The optimization of the retardance of the waveplates and the sampling scheme of (θ_1, θ_2) for efficient measurements of M is the subject in the followings.

Let's write equation (4) with matrix elements as

$$m_i = \sum_{k=1}^{N} r_{ik} I_k, \qquad i = 1 \sim 16$$

and assume, for simplicity, that the random noise in measurement of intensity, δI_k, does not change for each measurement (not dependent on k). Then the propagation of the error into m_i can be evaluated as

$$\delta m_i{}^2 = \delta I^2 \sum_{k=1}^{N} r_{ik}{}^2$$

(5)

If we denote the error in determining the intensity I from N-times measurements as $\delta I' = N^{-1/2}\,\delta I$, then equation (5) can be written as

$$\frac{\delta I'}{\delta m_i} = \left(N \sum_{k=1}^{N} r_{ik}{}^2 \right)^{-\frac{1}{2}} \equiv E_i \qquad (6)$$

Since the error of m_i (δm_i) gets smaller with respect to the error of intensity ($\delta I'$) when E_i, gets larger, E_i is regarded as 'efficiency of measurement' for the Mueller matrix element m_i.

To find the optimized retardation of the waveplates, we calculate Ei in a case of an uniform sampling for both θ_1 and θ_2 by a step of 22.5° and $\delta_1 = \delta_2 \equiv \delta$. Figure 3 shows E_i's for 16 elements of **M** as a function of δ. It is obvious that the peak of the efficiencies differ for the different elements of the Mueller matrix; the efficiencies for i =1~3 and j =1~3 elements have a peak at δ=180°, while efficiencies for i =4 or j =4 elements have peaks in δ =90~130°. Retardation in a range of 90~150°. would be fine for determining the all elements and nearly equal efficiencies among all elements can be achieved when the retardation is about 127°.

In the followings of this paper, we consider a system in which both waveplates rotate continuously with a constant ratio of speeds, $\dot{\theta}_1 = r\dot{\theta}_2$ or $\omega_1 = r\omega_2$. Such system is favorable for a simple and fast acquisition of data in actual hardware. The efficiency of measurement is a function of only the ratio of the speed, r, if the sampling rate of the intensity measurement is high enough. To find the optimized ratio of rotation speeds, we calculate the determinant of $C^t C$ as a function of r. The result for a case of $\delta_1 = \delta_2 = 127°$ is shown in figure 4, in which the minimum value of the efficiency E_i among 16 elements is also plotted by dashed curve. Both curves show a consistent result and we can notice that an efficient measurement of the Mueller matrix is achieved at the ratio of rotation speeds of 2.5, 3.5, 4.5, 5 and higher.
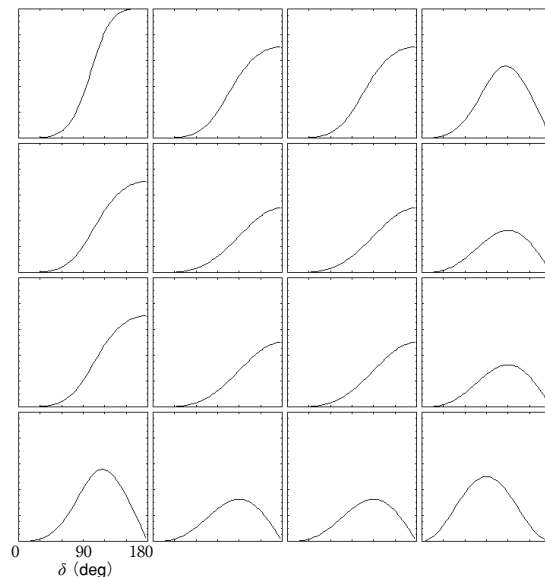

Figure 3. Efficiency of measurement for 16 Mueller matrix elements against the retardation of the waveplates.
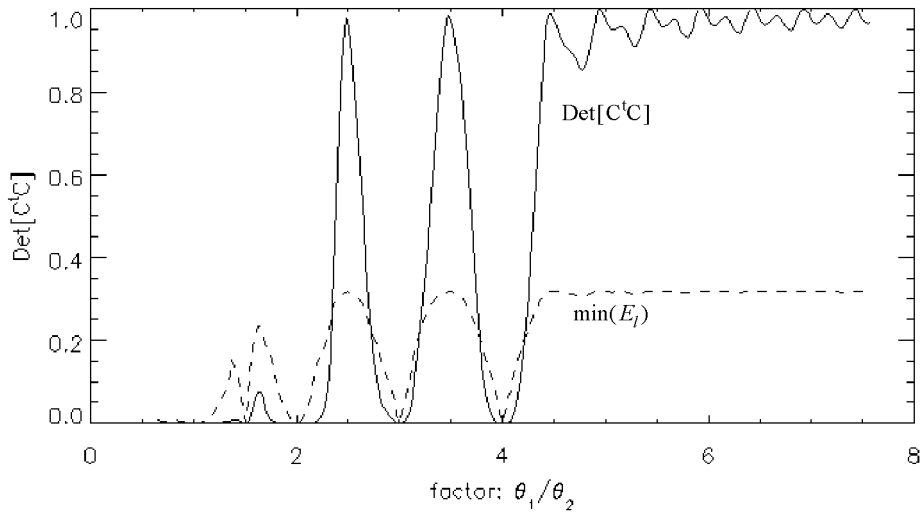
Figure 4. Determinant of CtC (solid curve) and minimum value of the efficiency E_i ($i = 1–16$)(dashed curve) as a function of the ratio of rotation speeds of the two waveplates.

3. Description of the Constructed Mueller Matrix Measurement System

3.1. Optical Setup

Figure 5 shows the setup of the constructed Mueller matrix measurement system. For the polarization analyzer, a Wollaston prism is used which has a separation angle between two beams of 20° (− 8.00°, 11.66° for each beam), and two orthogonally polarized lights are detected simultaneously by two photo diode sensors named as a and b. With this configuration, the accumulated photon is increased twice and the measurement error due to possible fluctuations of the light source can be eliminated in data analysis. The orientation of the linear polarization of the Wollaston prism defines the frame of Q and U of the system. An interference bandpass filter is placed at the exit of the Wollaston prism to isolate the wavelength.

The light passing through the system is defined by a diaphragm located after the light source, and the following optics is designed to accommodate the beam without vignetting; for example, the photo sensors which have a sensitive area of 10mmx10mm cover the entire beam spot made by the diaphragm. The rotating waveplates in the polarization generator and the analyzer are 0th order waveplates with a thin quartz layer attached on substrate (BK7). The retarda-

tion is about 127° at λ630nm. They have a clear aperture of about 10mm and are mounted in rotary stages driven by stepping motors with an angle resolution of 0.02°/step. Each stage has an origin sensor which provides a bi-level signal to the control system when the rotor passes its 'origin'. To obtain sufficient light at the photo sensors, the light beam (ie. the image of the diaphragm after the light source) is focused on the rotating waveplates with two lenses, and the sample is placed in a collimated beam made by them. The area of illumination on the sample and the brightness on the sensors can be adjusted by a variable circular mask in the collimated beam. The light level is also adjustable by changing the diameter of the diaphragm after the light source or the voltage for the lamp. A linear polarizer is located before the rotating waveplate in the polarization generator with its axis oriented nearly horizontal (+Q direction). A mechanical shutter is used to take a dark level. The light source is a halogen lamp operated with a current stabilized DC power supplier.

The arms of the polarization generator and the polarization analyzer are assembled on separate optical rails, and by arranging the locations of these arms, it is possible to measure the Mueller matrix of reflection as well. The polarization analyzer arm alone can also be used as a Stokes polarimeter. More detailed specifications of individual parts are described by Shinoda et al. (in preparation).
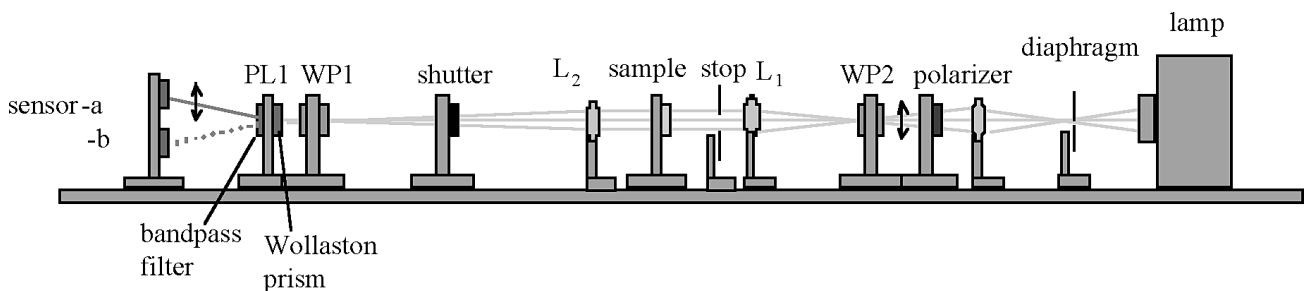

Figure 5. Optical setup of the system.

3.2. Formulation for Data Reduction

The intensities detected by the sensors a and b in our system are expressed by a slight extension of the equation (1) and (2),

$$I_{a,b}(\delta_1,\theta_1{}',\delta_2,\theta_2{}')=\alpha_{a,b}(1,0,0,0)\,\mathbf{PL}(\theta=0,\pi/2)\,\mathbf{WP}(\delta_1,\theta_1)\,\mathbf{M}'\,\mathbf{WP}(\delta_2,\theta_2)\,\mathbf{PL}(\theta=\theta_p)\,(1,0,0,0)^t$$

$$=\frac{1}{2}\alpha_{a,b}\sum_{k,l}c_{kl}^{a,b}(\theta_1,\theta_2)\,m_{kl} \qquad (7)$$

$$\theta_1{}'=\theta_1-d\theta_1, \qquad \theta_2{}'=\theta_2-d\theta_2$$

where $\alpha_{a,b}$ is the relative sensitivity of the two sensors, θ_p is the orientation of the polarizer in polarization generator (error in the setup), and $\theta_1{}', \theta_2{}'$ are the angles of rotors referring to their origin, and θ_1, θ_2 are the angles of the fast axis of waveplates with respect to +Q axis of the system which is defined by the Wallaston prism in the analyzer; $d\theta_1, d\theta_2$ are offset angles of the fast axes of the waveplates from the mechanical origins of the rotors. It is noticed that $\mathbf{M}'$ is not exactly the Mueller matrix of the sample, M, but is $\mathbf{M}'=L_1ML_2$, where L_1 and L_2 are Mueller matrices of the refocusing and collimating lenses between two waveplates. Since the two lenses are singlet without coating and due to the axi-symmetricity, L_1 and L_2 are expected to be close to the unit matrix.

In this paper, polarization elements (PL and WP) in the measurement system are assumed to be ideal ones. Propagation of errors from the imperfectness of components in the measurement system was studied by Nee (2003), and it is beyond the scope of this paper.

The 16×2 elements $c^{a,b}{}_{kl}$ in equation (7) are expressed as

$C_{11} = 1$

$C_{12} = (\text{ct}_2{}^2 + \text{cd}_2\,\text{st}_2{}^2)\,\text{ct}_p + (\text{ct}_2\,\text{st}_2 - \text{cd}_2\,\text{ct}_2\,\text{st}_2)\,\text{st}_p$

$C_{13} = (\text{ct}_2\,\text{st}_2 - \text{cd}_2\,\text{ct}_2\,\text{st}_2)\,\text{ct}_p + (\text{cd}_2\,\text{ct}_2{}^2 + \text{st}_2{}^2)\,\text{st}_p$

$C_{14} = \text{sd}_2\,\text{st}_2\,\text{ctp} - \text{sd}_2\,\text{ct}_2\,\text{st}_p$

$C_{21} = +/- (\text{ct}_1{}^2 + \text{cd}_1\,\text{st}_1{}^2)$

$C_{22} = +/- (\text{ct}_1{}^2 + \text{cd}_1\,\text{st}_1{}^2)(\text{ct}_2{}^2 + \text{cd}_2\,\text{st}_2{}^2)\,\text{ct}_p \;+/-\; (\text{ct}_1{}^2 + \text{cd}_1\,\text{st}_1{}^2)(\text{ct}_2\,\text{st}_2 - \text{cd}_2\,\text{ct}_2\,\text{st}_2)\,\text{st}_p$

$C_{23} = +/- (\text{ct}_1{}^2 + \text{cd}_1\,\text{st}_1{}^2)(\text{ct}_2\,\text{st}_2 - \text{cd}_2\,\text{ct}_2\,\text{st}_2)\,\text{ct}_p \;+/-\; (\text{ct}_1{}^2 + \text{cd}_1\,\text{st}_1{}^2)(\text{cd}_2\,\text{ct}_2{}^2 + \text{st}_2{}^2)\,\text{st}_p$

$C_{24} = +/- \text{st}_2\,\text{sd}_2\,(\text{ct}_1{}^2 + \text{cd}_1\,\text{st}_1{}^2)\,\text{ct}_p \;-/+\; \text{ct}_2\,\text{sd}_2\,(\text{ct}_1{}^2 + \text{cd}_1\,\text{st}_1{}^2)\,\text{st}_p$

$C_{31} = +/- (\text{ct}_1\,\text{st}_1 - \text{cd}_1\,\text{ct}_1\,\text{st}_1)$

$C_{32} = +/- (\text{ct}_1\,\text{st}_1 - \text{cd}_1\,\text{ct}_1\,\text{st}_1)(\text{ct}_2{}^2 + \text{cd}_2\,\text{st}_2{}^2)\,\text{ct}_p \;+/-\; (\text{ct}_1\,\text{st}_1 - \text{cd}_1\,\text{ct}_1\,\text{st}_1)(\text{ct}_2\,\text{st}_2 - \text{cd}_2\,\text{ct}_2\,\text{st}_2)\,\text{st}_p$

$C_{33} = +/- (\text{ct}_1\,\text{st}_1 - \text{cd}_1\,\text{ct}_1\,\text{st}_1)(\text{ct}_2\,\text{st}_2 - \text{cd}_2\,\text{ct}_2\,\text{st}_2)\,\text{ct}_p \;+/-\; (\text{ct}_1\,\text{st}_1 - \text{cd}_1\,\text{ct}_1\,\text{st}_1)(\text{cd}_2\,\text{ct}_2{}^2 + \text{st}_2{}^2)\,\text{st}_p$

$C_{34} = +/- \text{st}_2\text{sd}_2\,(\text{ct}_1\,\text{st}_1 - \text{cd}_1\,\text{ct}_1\,\text{st}_1)\,\text{ct}_p \;-/+\; \text{ct}_2\,\text{sd}_2\,(\text{ct}_1\,\text{st}_1 - \text{cd}_1\,\text{ct}_1\,\text{st}_1)\,\text{st}_p$

$C_{41} = -/+ \text{sd}_1\,\text{st}_1$

$C_{42} = -/+ \text{sd}_1\,\text{st}_1\,(\text{ct}_2{}^2 + \text{cd}_2\,\text{st}_2{}^2)\,\text{ct}_p \;-/+\; \text{sd}_1\,\text{st}_1\,(\text{ct}_2\,\text{st}_2 - \text{cd}_2\,\text{ct}_2\,\text{st}_2)\,\text{st}_p$

$C_{43} = -/+ \text{sd}_1\,\text{st}_1\,(\text{ct}_2\,\text{st}_2 - \text{cd}_2\,\text{ct}_2\,\text{st}_2)\,\text{ct}_p \;-/+\; \text{sd}_1\,\text{st}_1\,(\text{cd}_2\,\text{ct}_2{}^2 + \text{st}_2{}^2)\,\text{st}_p$

$C_{44} = -/+ \text{sd}_1\,\text{sd}_2\,\text{st}_1\,\text{st}_2\,\text{ct}_p \;+/-\; \text{sd}_1\,\text{sd}_2\,\text{st}_1\,\text{ct}_2\,\text{st}_p \qquad (8)$

where,

$\text{sd}_1 = \sin\delta_1, \quad \text{cd}_1 = \cos\delta_1, \quad \text{st}_1 = \sin2\theta_1, \quad \text{ct}_1 = \cos2\theta_1,$
$\text{sd}_2 = \sin\delta_2, \quad \text{cd}_2 = \cos\delta_2, \quad \text{st}_2 = \sin2\theta_2, \quad \text{ct}_2 = \cos2\theta_2,$
$\text{st}_p = \sin2\theta_p, \quad \text{ct}_p = \cos2\theta_p$
and $\pm$ stands for the sensors a and b.

To calculate the Mueller matrix of the sample (**M**) with equation (4), we need to determine the 7 unknowns, $\alpha_{a,b}$, δ_1, δ_2, $d\theta_1$, $d\theta_2$, and θp. This is performed by measuring the intensity modulation without the sample in the beam ('clear' measurement). In this case (**M**=**E**, where **E** is 4×4 unit matrix), assuming that $\mathbf{M}' = L_1L_2 = \mathbf{E}$, we obtain the following equation;

$$\begin{aligned} I_{a,b} &= \alpha_{a,b}\,[\;C_{11} + C_{22} + C_{33} + C_{44}\;] \\ &= \alpha_{a,b}\,[\;1 +/- (1+\text{cd}_1)(1+\text{cd}_2)\text{ct}_p/4 \\ &\quad +/- (1-\text{cd}_1)(1+\text{cd}_2)\cos(4\theta_1 - 2\theta_p)/4 \\ &\quad +/- (1+\text{cd}_1)(1-\text{cd}_2)\cos(4\theta_2 - 2\theta_p)/4 \\ &\quad +/- (1-\text{cd}_1)(1-\text{cd}_2)\cos(4(\theta_1 - \theta_2) + 2\theta_p)/4 \\ &\quad -/+ \text{sd}_1\,\text{sd}_2[\cos2(\theta_1 - \theta_2 + \theta_p) - \cos2(\theta_1 + \theta_2 - \theta_p)]/2\;]\;(9) \end{aligned}$$

When two waveplates rotate at constant angular speeds ($\theta_1 = \omega_1 t$ and $\theta_2 = \omega_2 t$), modulation amplitudes of I_a and I_b in frequencies $4\omega_1$, $4\omega_2$, $4(\omega_1 - \omega_2)$, $2(\omega_1 - \omega_2)$, $2(\omega_1 + \omega_2)$ are proportional to α_a and α_b. We denote the average of these amplitudes as A_a and A_b, respectively, and define a constant number α as

$$\frac{I_a(t)}{A_a} + \frac{I_b(t)}{A_b} \equiv 2\alpha$$

Then the normalizations

$$\frac{I_a(t)}{A_a\alpha} \equiv \bar{I}_a(t), \qquad \frac{I_b(t)}{A_b\alpha} \equiv \bar{I}_b(t) \qquad (10)$$

give $\bar{I}_a(t) + \bar{I}_b(t) = 2$ and thus two of the 7 unknowns are obtained as $\alpha_{a,b} = A_{a,b}\,\alpha.$. Hereafter, we denote the modulation amplitudes of the normalized I_a and I_b as $A_a(\omega)$ and $A_b(\omega)$.

From equation (9) we obtain a set of equations relating the amplitudes of the Fourier components and retardation of the waveplates,

$$4A_a(4\omega_1) = 4A_b(4\omega_1) = (1-\cos\delta_1)(1+\cos\delta_2) = \text{mp}, \qquad (11\text{-}1)$$
$$4A_a(4\omega_2) = 4A_b(4\omega_2) = (1+\cos\delta_1)(1-\cos\delta_2) = \text{pm}, \qquad (11\text{-}2)$$
$$4A_a(4(\omega_1-\omega_2)) = 4A_b(4(\omega_1-\omega_2)) = (1-\cos\delta_1)(1-\cos\delta_2) = \text{mm}, \quad (11\text{-}3)$$
$$2A_a(2(\omega_1-\omega_2)) = 2A_b(2(\omega_1-\omega_2)) = 2A_a(2(\omega_1+\omega_2))$$
$$= 2A_b(2(\omega_1+\omega_2)) = \sin\delta_1\sin\delta_2 = \text{ss}, \qquad (11\text{-}4)$$

In equations (11), δ_1 and δ_2 are overdetermined. From equations (11-1) and (11-3) or (11-2) and (11-3),

$$\cos\delta_1 = 1 - (\text{mp+mm})/2$$
$$\cos\delta_2 = 1 - (\text{pm+mm})/2$$

The combination of equations (11-1) and (11-2) also gives the following relation,

$$\cos^2\delta_1 + (\text{mp}-\text{pm})/2\;\cos\delta_1 + (\text{mp+pm})/2 - 1 = 0.$$

We adopt the mean value of δ_1 and δ_2 calculated from these equations.

By denoting the phases of the Fourier components of

$4\omega_1$, $4\omega_2$, and $4(\omega_1-\omega_2)$ as ϕ_1, ϕ_2, and ϕ_d, respectively, we obtain another set of equations for the phases from equation (9);

$$\phi_1 = 4d\theta_1 + 2\theta_1$$
$$\phi_2 = 4d\theta_2 + 2\theta_p$$
$$\phi_d = 4(d\theta_1 - d\theta_2) - 2\theta_p$$

and following relations are derived.

$$d\theta_1 = (\phi_d + \phi_2)/4$$
$$\theta_p = (\phi_1 - \phi_2 - \phi_d)/2 = (\phi_1 - 4d\theta_1)/2$$
$$d\theta_2 = (\phi_1 - \phi_d - 4\theta_p)/4 = (\phi_2 - 2\theta_p)/4$$

When we have multiple ways to calculate the unknowns, we again adopt the average value of them. Thus all 7 parameters (a_a, a_b, δ_1, δ_2, $d\theta_1$, $d\theta_2$, and θp) can be determined from the 'clear' measurement. By applying equation (4) on I_a and I_b of the clear measurement with C calculated from equation (8), we obtain a Mueller matrix of the 'clear', which would represent $\mathbf{M}' = \mathbf{L}_1\mathbf{L}_2$.

The measurement of the sample with the following application of equations (8) and (4) to the obtained I_a and I_b gives the Mueller matrix of the sample with a possible modification by the two lenses, i.e., $\mathbf{M}' = \mathbf{L}_1\mathbf{M}\mathbf{L}_2$. Since $\mathbf{L}_1$ and $\mathbf{L}_2$ are close to the unit matrix, we can denote $\mathbf{L}_1 = \mathbf{E} + \mathbf{l}_1$, $\mathbf{L}_2 = \mathbf{E} + \mathbf{l}_2$, where E is the unit matrix and $\mathbf{l}_1$ and $\mathbf{l}_2$ are matrices with elements of small number ($\ll 1$). Then,

$$\mathbf{M}' = \mathbf{L}_1\mathbf{M}\mathbf{L}_2 = (\mathbf{E}+\mathbf{l}_1)\,\mathbf{M}\,(\mathbf{E}+\mathbf{l}_2) \sim \mathbf{M} + \mathbf{l}_1\,\mathbf{M} + \mathbf{M}\,\mathbf{l}_2 \quad (12)$$

When the sample is a weak polarization element, i.e., $\mathbf{M} \sim \mathbf{E} + \mathbf{m}$, equation (12) is

$$\mathbf{M}' \sim \mathbf{E} + \mathbf{m} + \mathbf{l}_1 + \mathbf{l}_2,$$

after neglecting the second order infinitesimals. The error of measurement is thus about $\mathbf{l}_1 + \mathbf{l}_2$. On the other hand, if we apply the inverse of the 'clear' matrix on the obtained Mueller matrix,

$$(\mathbf{L}_1\mathbf{L}_2)^{-1}\,\mathbf{M}' = \mathbf{L}_2^{-1}\mathbf{M}\mathbf{L}_2 \sim (\mathbf{E}-\mathbf{l}_2)\,\mathbf{M}\,(\mathbf{E}+\mathbf{l}_2) \sim \mathbf{M} - \mathbf{l}_2\,\mathbf{M} + \mathbf{M}\,\mathbf{l}_2$$
$$\sim \mathbf{E} + \mathbf{m} - \mathbf{l}_2\,\mathbf{m} + \mathbf{m}\,\mathbf{l}_2 \sim \mathbf{E} + \mathbf{m} \sim \mathbf{M}.$$

Thus the correction with the 'clear' matrix gives a better evaluation of the sample matrix if the sample is a weakly polarizing element, and we apply this correction in the standard procedure of the measurement. It is noted that the direction of multiplication of $(\mathbf{L}_1\mathbf{L}_2)^{-1}$ on $\mathbf{M}'$ is not matter in this approximation.

It is noted that all quantities used for data reduction are derived from amplitude and phase of the Fourier components at frequencies of $4\omega_1, 4\omega_2, 4(\omega_1-\omega_2), 2(\omega_1-\omega_2)$, and $2(\omega_1+\omega_2)$. If these frequencies are not equal to ω_1 nor ω_2 (this is the case for actual operation), undesired intensity modulations at frequencies of ω_1 or ω_2 which may be caused by beam wobbling in the optical path due to the rotating waveplates do not affect the measurement results. It is also recognized that the operation of eq. (4) is essentially extracting the Fourier components other than the frequencies

of ω_1 or ω_2. The higher harmonic terms of such modulation are still possible error sources of the system.

3.3. Control and Operation of the System

Figure 6 shows the block diagram of the measurement system. Two rotary stages are driven by a 2-axis motor driver controlled from a PC via a serial interface. We adopt the ratio of the rotation speed of the waveplate-1 and -2 of 5:1, which is one of the efficient ratio as discussed in section 2. The rotation rate of the waveplate-1 is 3 rev/sec, thus a complete set of data is obtained in 1.67sec. (1 revolution of the waveplate-2). The signal from the photo sensors a and b, and two origin sensors of the rotors are digitized by a 16 bit AD conversion card in 10.8kHz, thus the angle resolution for the waveplate-1 is 0.1deg.
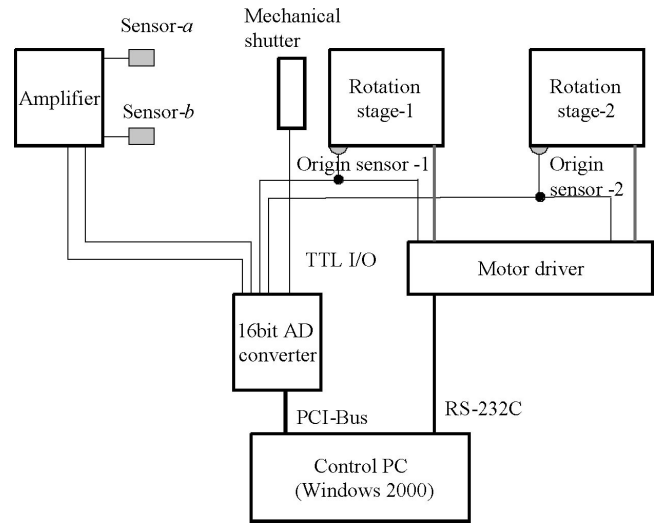

Figure-6. Block diagram of the system.

At the beginning of measurements, dark levels are taken with the sensors a and b by closing the mechanical shutter. Then the 'clear' measurement is performed to obtain the parameters, $a_{a,b}$, δ_1, δ_2, $d\theta_1$, $d\theta_2$, and θ_p, for the use in following analyses. In usual measurements, data is recorded continuously during a period containing at least three passages of the mechanical origin of the rotation stage-2. By sensing the edges of the origin sensor signals of the waveplate 1 and 2, angles of waveplates referring to the mechanical origin, θ_1' and θ_2', at each data point are determined, and then data with 0.1deg resolution for WP-1 is binned 10 times to reduce the amount of data to be stored in hard disk (at this point, the array contains about 4000 data points with a resolution of 1deg. for WP-1). Data analysis is immediately made to determine the 7 parameters for 'clear' measurements, or the Mueller matrix of the sample for sample measurements. In sample measurements, amounts of the retardation, diattenuation and depolarization and their eigen polarizations are calculated from the obtained Mueller matrix by using the decomposition algorithm given by Lu and Chipman (1996).
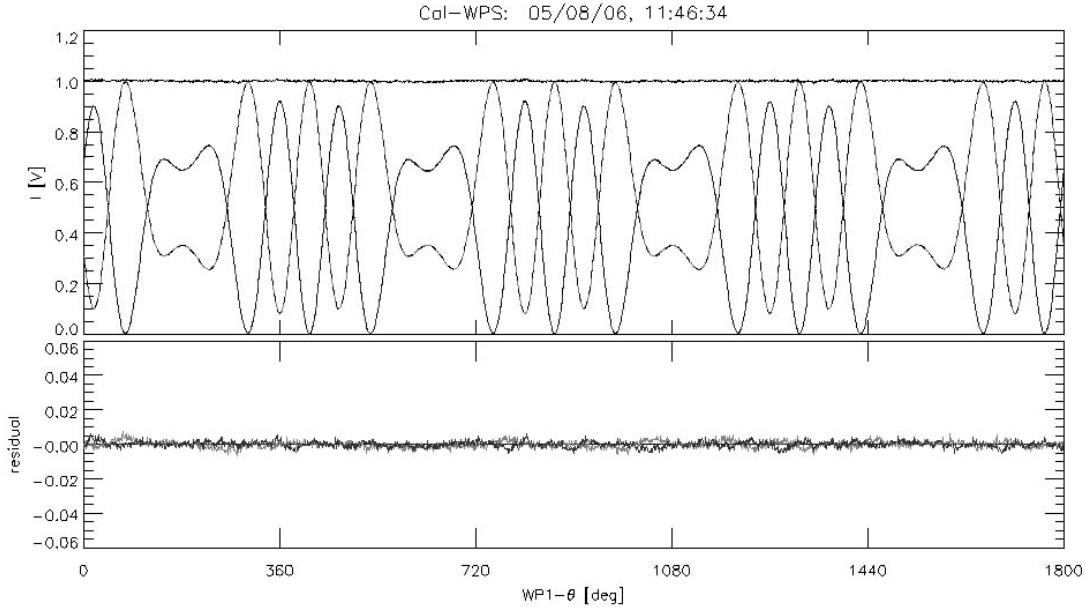
Figure 7. An example of normalized intensity modulation profiles I_a and I_b in a clear measurement as a function of the angle of the waveplate-1 (top). The bottom curves show residuals of fitting by the theoretical curve with the derived parameters. This plot is obtained at 633nm, where the derived retardation of the waveplates, δ_1 and δ_2, are both 125.6 deg.

4. Examples of Measurements

4.1. Clear

Figure 7 shows an example of intensity modulation profiles, I_a and I_b (normalaized by equation (10)), as a function of the angle of the waveplate-1 in a clear measurement. The theoretical curves of equation (7) using the derived 7 parameters fit the observed intensity variation fairly well as shown in the bottom curves. The Mueller matrix of the 'clear' is shown below. The repeatability of measurements is of the order of 3×10^{-4} for each matrix elements, and the deviation of the Mueller matrix of 'clear' from the unit matrix cannot be attributed to the random noise. It is supposed that the two lenses in the optical path contribute to this deviation.

Mueller matrix from a 'clear' measurement

0.9998,	0.0009,	$-0.0004,$	0.0003
$-0.0017,$	0.9991,	0.0001,	0.0006
$-0.0001,$	$-0.0006,$	0.9978,	0.0015
0.0005,	0.0033,	$-0.0004,$	0.9807

4.2. Polarizers (Strong Polarization Element)

We present the results of measurement of 3 types of sheet polarizer of 3M Corporation; HN38 (linear polarizer), HNCP37R (right hand circular polarizer), and HNCP37L (left hand circular polarizer), which are used to characterize the polarization property of the Solar Optical Telescope (SOT) onboard the Solar-B (Ichimoto etal, 2004). In the

HN38 (measurement on 2004.9.14)

1.0000	0.9916	0.0000	0.0025
0.9989	0.9969	0.0000	0.0022
0.0145	0.0145	0.0000	-0.0003
0.0000	0.0008	0.0003	-0.0006

transmission=   0.358

standard deviation of 4 orientations

0.0000	0.0030	0.0000	0.0052
0.0027	0.0053	0.0003	0.0052
0.0038	0.0039	0.0001	0.0002
0.0069	0.0075	0.0032	0.0003

HNCP37R (measurement on 2005.6.10)

1.0000	0.9866	0.0000	0.0428
0.1052	0.1047	0.0000	0.0043
-0.1064	-0.1057	0.0000	-0.0044
0.9811	0.9763	0.0001	0.0425

transmission=   0.346

standard deviation of 4 orientations

0.0000	0.0058	0.0000	0.0016
0.0056	0.0064	0.0005	0.0003
0.0083	0.0081	0.0003	0.0003
0.0005	0.0062	0.0004	0.0015

HNCP37L (measurement on 2005.6.10)

1.0000	0.9868	0.0000	-0.0432
0.0032	0.0034	0.0002	-0.0001
-0.0636	-0.0633	0.0001	0.0027
-0.9905	-0.9853	-0.0002	0.0430

transmission=   0.354

standard deviation of 4 orientations

0.0000	0.0054	0.0000	0.0020
0.0019	0.0021	0.0002	0.0002
0.0035	0.0037	0.0003	0.0002
0.0003	0.0061	0.0003	0.0020

measurements of Mueller matrix, a piece of sheet polarizer was set at 4 orientations successively with its axis in approximately 0, 45, 90, and 135 deg. The obtained Mueller matrices in different orientations are rotated to make (1,3) element 0 and averaged. Results are shown below with the standard deviation among the 4 measurements in the right.

General characteristics of a linear diattenuator or circular polarizer are evident in each Mueller matrix, while the standard deviation on the right gives an idea of amount of the orientation-dependant systematic error in the measurement.

4.3. A Lens (Weak Polarization Element)

The astigmatism corrector lens used in SOT is a nearly plane parallel plate to eliminate a small, as-built aberration of the optics. The lens is bonded in a titanium cell with adhesive at 3 points near the edge. The polarization property of this lens was examined with a special attention paid on its temperature-dependent retardation caused by the mechanical stress from the mount. Two different areas of the lens were measured, namely, at the edge near the mounting point and the center of the lens. Since observed Mueller matrices have no significant change from the unit matrix except the linear retardation, we give only (3,4) element of the observed Mueller matrix as a function of the temperature of lens in figure 8. It is obvious that the (3,4) element (=linear retardation) near the mounting point changes significantly with the temperature, while the retardation at the center of the lens is much smaller and constant.
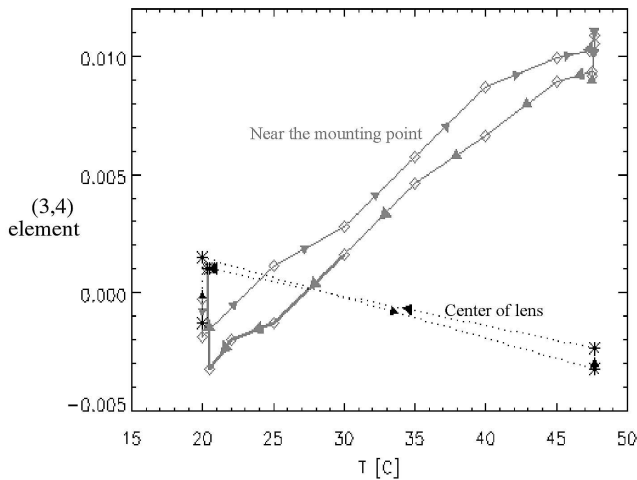

Figure 8. (3,4) element of the Muller matrix of the astigmatism corrector lens of SOT as a function of temperature. The curve with diamond is for the edge near the mounting point and the curve with asterisk is for center of the lens.

These results imply that the measurement system is sensitive to the weak retardation of the order of 0.001 or less. A representative Mueller matrix for the center of the lens at T=20C is shown together with the corresponding diattenuation and retardation. It is notable that the repeatability of measurement is quite good to the order of 3×10^{-4} for each Mueller matrix element.

Mueller matrix of the lens at the center and T=20C

$$
\begin{array}{rrrr}
0.9911, & 0.0001, & 0.0002, & -0.0002 \\
-0.0000, & 0.9918, & -0.0004, & 0.0024 \\
-0.0001, & 0.0003, & 0.9917, & 0.0014 \\
0.0000, & -0.0013, & -0.0009, & 0.9899
\end{array}
$$

Diattenuation.: 0.0003, Retardation: 0.13deg.

4-4. KD*P (Variable Strong Retarder)

The Mueller matrix of the KD*P variable retarder used as a polarization modulator of the Solar Flare Telescope at Mitaka (Sakurai etal, 1995) was measured. This KD*P consists of 2 KD*P crystals layers with a half waveplate in between them and the retardation can be controlled in a range of ~ ± half wave at 630nm by changing the applying voltage. Figure 9 shows the obtained variations of the Mueller matrix elements against the voltage (diamond).
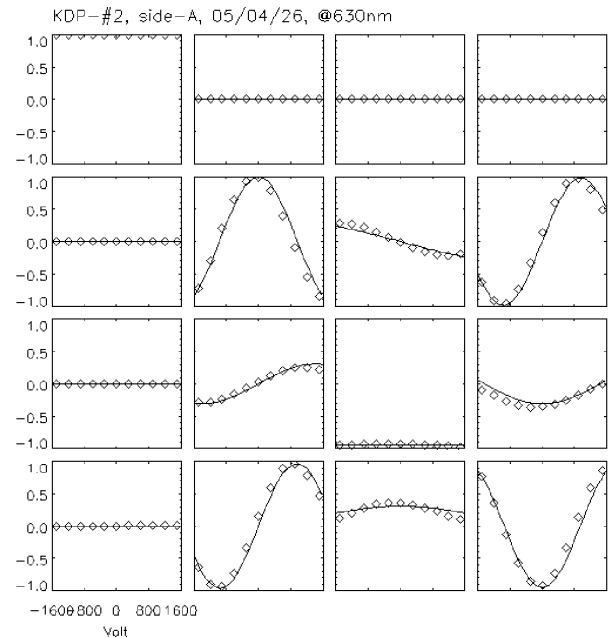

Figure 9. 16 Mueller matrix elements of KD*P as a function of applied voltage. Symbols are measurement, solid curves are model fitting with a retardation of central waveplate of 198°.

It is clear that (2,4) and (4,2) elements show a large variation with the voltage as expected and the Mueller matrix can entirely convert ± V to +Q at certain voltages (= operation voltages for this device). On the other hand, (2,3), (3,2), (3,4), (4,3) elements are expected to be constant, but it is not the case. This behavior can be understood if the retardation of the 'half' waveplate sandwiched by the two KD*P layers is not exactly at half wave at the measurement wavelength; the observed variation can be explained if we assume the retardance of the waveplate to be 198° (solid curves).

5. Conclusion

A photopolarimetric measurement system of the Mueller matrix of optical elements is constructed with dual rotating waveplates. This system enables us to evaluate the polarization properties of optical elements for various

polarimetric observation systems in a simple and quick manner. The repeatability of measurement is as high as a few $\times$ 10^{-4} for each element of the Mueller matrix, and the system is sensitive to $<10^{-3}$ for the Mueller matrix elements of weak polarization elements. On the other hand, the nature of possible systematic errors for the strong polarization element is not absolutely known, and remains as a further subject to be explored.

References
Azzam, R.M.A., 1978, Photopolarimetric measurement of the Mueller matrix by Fourier analysis of a single detected signal. *Optics Letters*, **2**, 148 – 150.
Collins, R.W., and Koh, J., 1999, Dual rotating-compensator multichannel ellipsometer: instrument design for real-time Mueller matrix spectroscopy of surfaces and films. *J.Opt.Soc.Am.A*, **16**, 1997 – 2006.
Goldstein, D.H., 1992, Mueller matrix dual-rotating retarder polarimeter. *Appl.Optics*, **31**, 6676 – 6683.
Ichimoto,K., Tsuneta,S., Suematsu,Y., etal., 2004, The Solar Optical Telescope onboard the Solar-B. *Proceedings of SPIE*, **5487**, 1142 – 1151.
Lu, S.Y., and Chipman, R.A., 1996, An interpretation of Mueller matrices based on the polar decomposition. *J.Opt.Soc.Am.A,* **13**, 1106 – 1113.
Makita, M., Hamana, S., Kawakami, H., Nishi, K., 1982, *Annals of Toyko Astronomical Observatory*, **19**, 24 – 37.
Nee, S.F., 2003, Error analysis for Mueller matrix measurement. *J.Opt.Soc.Am.A*, **20**, 1651 – 1657.
Sakurai,T., Ichimoto,K., Nishino,Y., etal., 1995, Solar Flare Telescope at Mitaka. *PASJ*, **47**, 81 – 92.
Shinoda,K., etal, 2006, in preparation.